Novel Adenine/Thymine Photodimerization channels mapped by PCM/TD-DFT calculations on dApT and TpdA dinucleotides.

Lara Martínez-Fernández[a] *and Roberto Improta*[*a].

Supporting Information **Pages**

1. Further Computational Details 2

2. Further Results

   2.1. Structural Analysis

      2.1.1. Syn-Anti Equilibirum 2

      2.1.2. Stacked/Unstacked 3

   2.2. The Franck-Condon region

      2.2.1. Absorption Spectra 4-5

      2.2.2. Circular Dichroism Spectra 5

   2.3. HOMO and LUMO orbitals 6

1. Further Computational Details

The ground (S_0) and excited state (S_1) of the dApT and TpdA dinucleotides have been optimized using Density Functional Theory (DFT) and its Time Dependent version (TD-DFT), respectively.

We have selected the M052X[1] functional since it has been already successfully applied in the study of the dinucleotides photodimerization (adenine-adenine and thymine-thymine)[2] as well as of the DNA photophysics.[3] Due to the incorporation of 'ad hoc' corrections for both dispersion interactions and Charge Transfer transitions, M052X improves the results given by the "standard" functionals for the study of stacked multi-chromophore systems. The 6-31G(d) basis set was used for all calculations. Solvent (water) effect has been included using the Polarizable Continuum Model (PCM)[4] and exploiting the 'standard' LR (linear-response) implementation of PCM/TD DFT, for which analytic gradients are available.[5] State Specific (SS)[6]/PCM single point calculations were performed at extracted geometries of the different relaxed scans in order to better estimate the role of solvent dynamics. The single points were performed both considering that the solvent is not completely equilibrated to the excited state density (non-equilibrium, neq) and considering fully equilibration (equilibrium, eq).

Gaussian09 package was used for these calculations.[7]

2. Additional Results

2.1. Structural Analysis

Syn-Anti Equilibirum

A detailed analysis regarding the syn-anti equilibrium can be found in the main text.

Scheme S1. Anti-Anti and Syn-Anti conformers for the dApT and TpdA dinucleotides, including atom labeling.

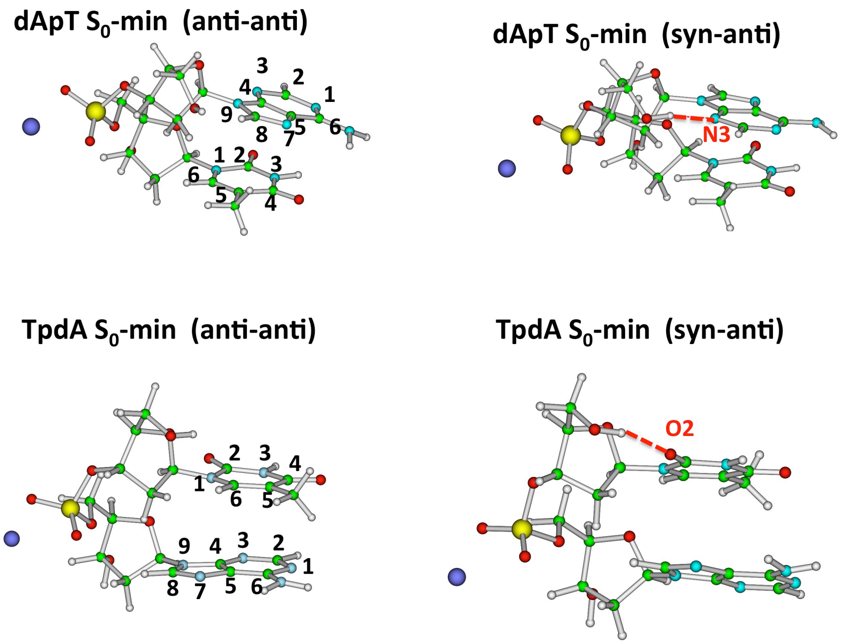
dApT S_0-min (anti-anti)

dApT S_0-min (syn-anti)

TpdA S_0-min (anti-anti)

TpdA S_0-min (syn-anti)

Stacked/Unstacked

Another debated issue concerns the degree of interbase stacking in dApT and TpdA dinucleotides. Besides the global stacked minima, we have then optimized a fully unstacked conformation (Unstacked-2), where the two bases are almost perpendicular, together with an intermediate situation (Unstacked-1), see Figure S1. For dApT the three geometries correspond all to relative minima on S_0. For TpdA the totally unstacked-2 geometry decays to the global unstacked-1 minimum. Although it has been stated[8] that dApT prefers unstacked conformations, our calculations (Table S1) indicate instead that the stacked minimum is the most stable one in this case. TpdA unstacked-1 is however more stable, which could be due in part to the presence of a H-bond between the carbonyl group of Thy and the NH_2 group of Ade. In any case, the energy of the different minima is similar, and a complete dynamical study would be necessary to firmly assess the conformational behavior of dApT and TpdA. This is outside the scope of the present paper, also considering that the available force fields are likely not accurate enough for studying Single Strand oligonucleotides with the necessary degree of accuracy.[9] However, the present results suffice to show that it cannot be taken for granted that dApT is poorly stacked. Actually, available experimental results[10] and the following analysis of CD spectra support quite the opposite conclusion.

Table S1. Energies (in eV/kcal mol^{-1}) for the dApT and TpdA minima presenting different stacking rearrangements between bases optimized at the PCM-M052X/6-31G(d) level of theory.

	Stacked-1	Unstacked-1	Unstacked-2
dApT	0.00	0.14 / 3.22	0.02 / 0.42
TpdA	0.00	-0.15 / -3.45	0.04 / 1.02

Figure S1. dApT and TpdA minima presenting different stacking rearrangements between bases optimized at the PCM-M052X/6-31G(d) level of theory.

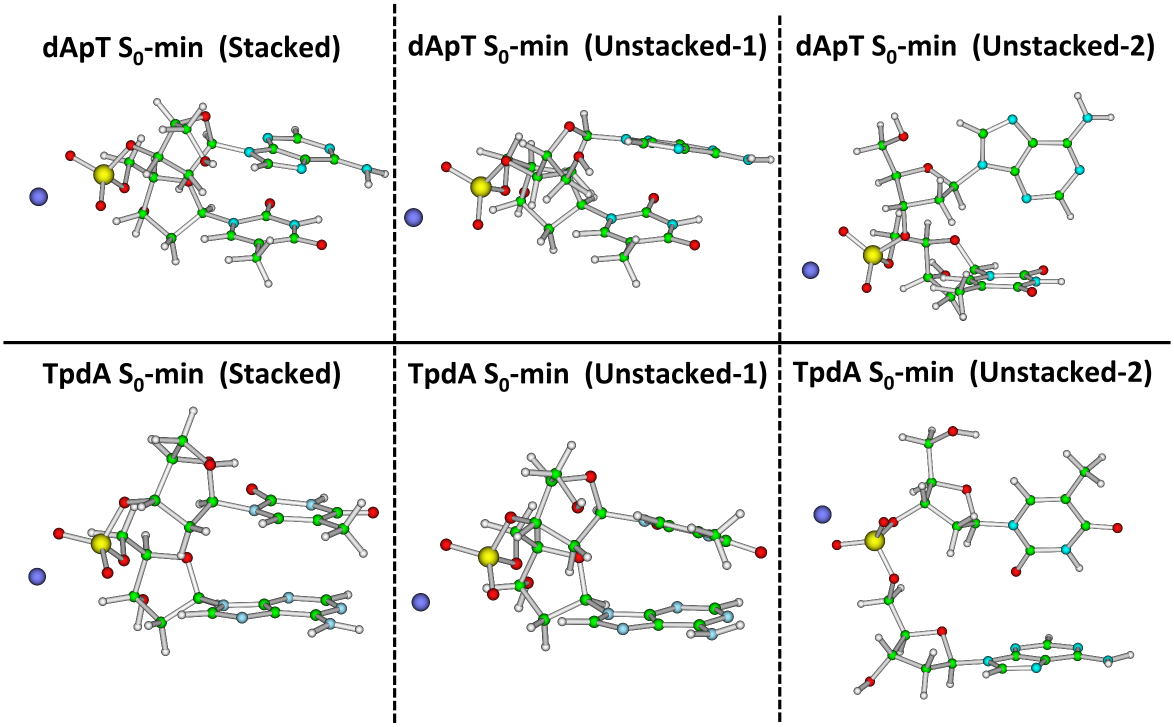

2.2. The Franck-Condon Region

2.2.1. Absorption Spectra

The absorption energies and oscillator strengths of the 6 lowest energy excited state calculated at the S_0-min (for both dApT and TpdA dinucleotides) at the PCM/TD-M052X/6-31G(d) level of theory are collected in Table S2. We have checked the effect that increasing the basis set (6-31+G(d,p)) and considering explicit water molecules (dApT+9H_2O) have on the absorption spectra.

Basis set effect: When the basis set size increases, the energy gap between the S_1 ($n\pi^*$ transition) and S_2 ($\pi\pi^*$ transition) excited states decreases, and they become almost degenerated. The energy difference between the two lowest bright transitions does not significantly change.
Explicit water molecules effect: Inclusion of explicit water molecules leads to an increase of the interbase distance (C^{6T}-C^{4A} dApT= 3.73Å vs dApT+9H_2O=4.11Å) and to a small decrease of the energy gap between the two lowest bright transitions. As expected, $n\pi^*$ transitions are significantly destabilized.

Table S2. Main transition character, coefficients, energies and oscillator strength (in parenthesis) for the lowest energy excited states of dApT and TpdA computed at the specified level of theory.

	PCM/TD-M052X/6-31G(d)		PCM/TD-M052X/6-31+G(d,p)	
dApT	Excitation	DE, eV (f)	Excitation	DE, eV (f)
S_1	$LP_{T1}\pi_T^*$ 0.41 $LP_{T1}\pi_T^*$ 0.26	5.15 (0.000)	$\pi_T\pi_T^*$ 0.57 $\pi_{A1}\pi_T^*$ 0.37	5.18 (0.151)
S_2	$\pi_T\pi_T^*$ 0.57 $\pi_{A1}\pi_T^*$ -0.37	5.34 (0.162)	$LP_{T1}\pi_T^*$ 0.48 $LP_{T1}\pi_T^*$ 0.19	5.20 (0.004)
S_3	$\pi_{A1}\pi_{A1}^*$ 0.65	5.49 (0.375)	$\pi_{A1}\pi_{A1}^*$ 0.66	5.34 (0.426)
S_4	$LP_A\pi_{A1}^*$ 0.62	5.57 (0.029)	$\pi_T\pi_T^*$ -0.36 $\pi_{A1}\pi_T^*$ 0.58	5.49 (0.019)
S_5	$\pi_{A1}\pi_{A1}^*$ 0.37 $\pi_{A1}\pi_{A2}^*$ 0.58	5.61 (0.019)	$\pi_{A1}\pi_{A1}^*$ -0.32 $\pi_{A1}\pi_{A2}^*$ 0.47	5.55 (0.009)
S_6	$\pi_{A2}\pi_{A1}^*$ -0.32 $\pi_{A1}\pi_{A2}^*$ 0.58	5.64 (0.020)	$\pi_{A1}\pi_{A1}^*$ 0.55 $\pi_{A1}\pi_{A2}^*$ 0.34	5.56 (0.011)
dApT+9H_2O				
S_1	$\pi_T\pi_T^*$ 0.67	5.31 (0.158)	-	-
S_2	$\pi_{A1}\pi_{A1}^*$ 0.52 $\pi_{A1}\pi_T^*$ -0.31	5.41 (0.316)	-	-
S_3	$LP_{T1}\pi_T^*$ -0.32 $LP_{T2}\pi_T^*$ 0.31	5.42 (0.005)	-	-
S_4	$\pi_{A1}\pi_{A2}^*$ 0.44 $\pi_{A1}\pi_{A1}^*$ -0.39 $\pi_{A1}\pi_T^*$ -0.26	5.54 (0.193)	-	-
S_5	$\pi_{A1}\pi_T^*$ 0.57 $\pi_{A1}\pi_{A2}^*$ 0.36	5.60 (0.012)	-	-
S_6	$LP_A\pi_{A1}^*$ 0.54	5.89 (0.001)	-	-
TpdA				
S_1	$LP_T\pi_T^*$ 0.51 $LP_T\pi_{A1}^*$ -0.22	5.14 (0.000)	$\pi_T\pi_T^*$ 0.47 $\pi_{A1}\pi_T^*$ -0.43 $\pi_{A1}\pi_{A1}^*$ -0.22	5.12 (0.023)

S_2	$\pi_T\pi_T^*$ -0.44 $\pi_{A1}\pi_T^*$ 0.45 $\pi_{A1}\pi_{A1}^*$ 0.25	5.29 (0.014)	$LP_T\pi_T^*$ 0.51 $LP_T\pi_{A1}^*$ -0.22	5.20 (0.005)
S_3	$\pi_T\pi_T^*$ 0.49 $\pi_{A1}\pi_T^*$ 0.37 $\pi_{A1}\pi_{A1}^*$ 0.24	5.46 (0.48)	$\pi_T\pi_T^*$ 0.48 $\pi_{A1}\pi_T^*$ 0.42 $\pi_{A1}\pi_{A1}^*$ 0.25	5.29 (0.474)
S_4	$LP_A\pi_T^*$ 0.33 $LP_A\pi_{A1}^*$ 0.56	5.57 (0.001)	$\pi_{A1}\pi_{A1}^*$ 0.38 π_{A1}Ryd 0.45	5.53 (0.086)
S_5	$\pi_{A1}\pi_{A1}^*$ -0.33 $\pi_{A1}\pi_{A2}^*$ 0.52	5.64 (0.087)	$LP_A\pi_T^*$ 0.34 $LP_A\pi_{A1}^*$ 0.54	5.57 (0.000)
S_6	$\pi_{A1}\pi_T^*$ -0.38 $\pi_{A1}\pi_{A1}^*$ 0.49	5.75 (0.059)	$\pi_{A1}\pi_T^*$ -0.30 $\pi_{A1}\pi_{A1}^*$ 0.46	5.65 (0.067)

2.2.2. CD Spectra

In order to confirm our predictions regarding the syn/anti conformations and bases stacking (see section 2.1) we have computed the electronic circular dichroism (CD) spectra for dApT and TpdA, in order to compare it with the experimental one [ref[11]]. The computed spectra are depicted in Figure S2. The experimental CD spectrum of TpdA dinucleotide is very similar to that computed for the stacked minimum, being both the unstacked-1 and syn-anti minima spectra significantly shifted. This agreement confirms that the minimum we have considered when studying TpdA photochemistry is representative of the conformational ensembles and suggests that TpdA is mainly present in the anti-anti conformation. For dApT, instead, despite the shape of the computed and the experimental spectra are similar, the intensity of the band around ~240nm is underestimated. The intensity of this feature is larger for the syn-anti conformer. Interestingly, a hypothetical spectra simulated by using 50% stacked and 50% syn-anti computed one, perfectly matches the experimental spectrum. The computed CD spectrum for the unstacked-1 minimum presents a too large positive band below 190 nm. These findings confirm that stacked anti-anti and syn-anti conformers are likely in equilibrium for dApT dinucleotide.

Figure S2. CD spectra for dApT (black) and TpdA (red) for stacked (solid lines), unstacked-1 (lines-points) and syn-anti (dashed lines) conformations. Experimental spectra (purple crosses) extracted from refs[11] are included for comparison. In the case of dApT CD a 50-50 mix of stacked and syn-anti conformation is also included in black points.

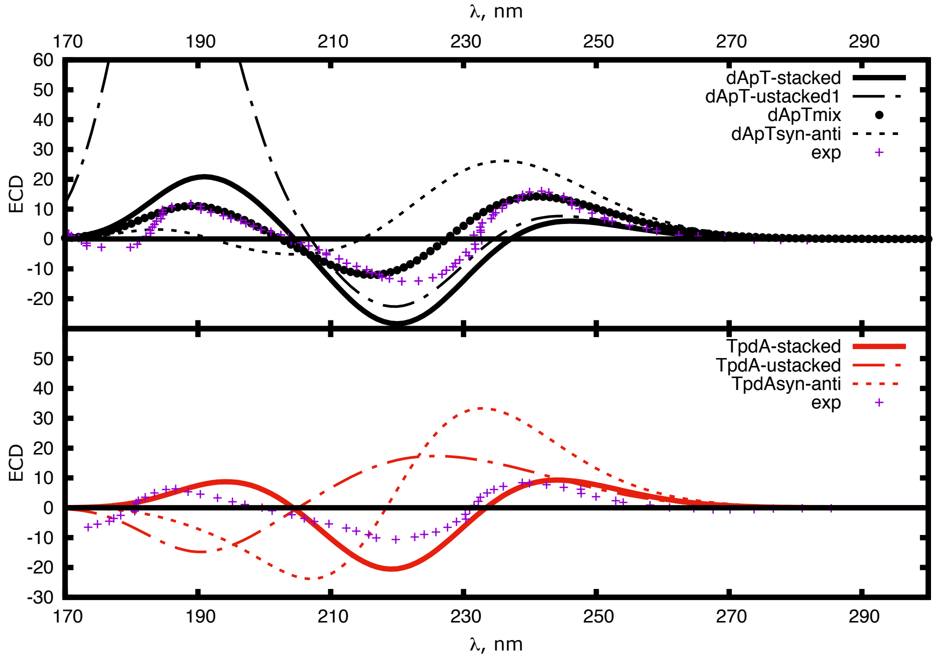

2.3. HOMO and LUMO orbitals

Figure S3. HOMO (H) and LUMO (L) Orbital involved in the H-L excitation at the dApT S_1-min calculated at the PCM-M052X/6-31G(d) level of theory.

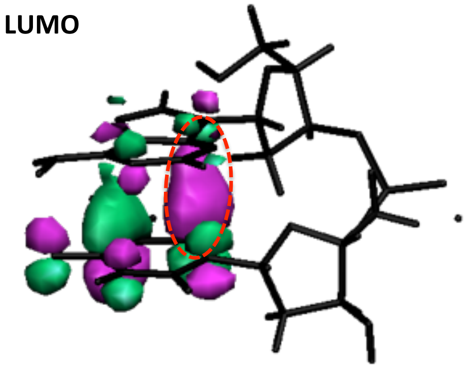

1. a)Y. Zhao, N. E. Schultz and D. G. Truhlar, *J. Chem. Theory Comput.*, 2006, **2**, 364; b)Y. Zhao and D. G. Truhlar, *Acc. Chem. Res.*, 2008, **41**, 157.
2. a)A. Banyasz, L. Martinez-Fernandez, T. Ketola, A. Muñoz-Losa, L. Esposito, D. Markovitsi and R. Improta, *J. Phys. Chem. Lett.*, 2016, **7**, 2020; b)A. Banyasz, T. Douki, R. Improta, T. Gustavsson, D. Onidas, I. Vayá, M. Perron and D. Markovitsi, *J. Am. Chem. Soc.* , 2012, **134**, 14834; c)L. Esposito, A. Banyasz, T. Douki, M. Perron, D. Markovitsi and R. Improta, *J. Am. Chem. Soc.*, 2014, **136**, 10838; d)R. Improta, *J. Phys. Chem. B*, 2012, **116**, 14261.
3. a)A. Banyasz, L. Esposito, T. Douki, M. Perron, C. Lepori, R. Improta and D. Markovitsi, *J. Phys. Chem. B*, 2016, **120**, 4232; b)F. J. Avila Ferrer, F. Santoro and R. Improta, *Comput. Theor. Chem.*, 2014, **1040–1041**, 186; c)R. Improta and V. Barone, *Theor. Chem. Acc.*, 2008, **120**, 491; d)R. Improta, *Chem. Eur. J.*, 2014, **20**, 8106.
4. a)S. Miertuš, E. Scrocco and J. Tomasi, *Chem. Phys.*, 1981, **55**, 117; b)J. Tomasi, B. Mennucci and R. Cammi, *Chem. Rev.*, 2005, **105**, 2999.
5. G. Scalmani, M. J. Frisch, B. Mennucci, J. Tomasi, R. Cammi and V. Barone, *J. Chem. Phys*, 2006, **124**, 094107.
6. a)R. Improta, G. Scalmani, M. J. Frisch and V. Barone, *J. Chem. Phys.*, 2007, **127**, 074504; b)R. Improta, V. Barone, G. Scalmani and M. J. Frisch, *J. Chem. Phys.*, 2006, **125**, 054103.
7. M. J. T. Frisch, G. W.; Schlegel, H. B.; Scuseria, G. E.; Robb, M. A.; Cheeseman, J. R.; Scalmani, G.; Barone, V.; Mennucci, B.; Petersson, G. A.; Nakatsuji, H.; Caricato, M.; Li, X.; Hratchian, H. P.; Izmaylov, A. F.; Bloino, J.; Zheng, G.; Sonnenberg, J. L.; Hada, M.; Ehara, M.; Toyota, K.; Fukuda, R.; Hasegawa, J.; Ishida, M.; Nakajima, T.; Honda,

Y.; Kitao, O.; Nakai, H.; Vreven, T.; Montgomery, Jr., J. A.; Peralta, J. E.; Ogliaro, F.; Bearpark, M.; Heyd, J. J.; Brothers, E.; Kudin, K. N.; Staroverov, V. N.; Kobayashi, R.; Normand, J.; Raghavachari, K.; Rendell, A.; Burant, J. C.; Iyengar, S. S.; Tomasi, J.; Cossi, M.; Rega, N.; Millam, N. J.; Klene, M.; Knox, J. E.; Cross, J. B.; Bakken, V.; Adamo, C.; Jaramillo, J.; Gomperts, R.; Stratmann, R. E.; Yazyev, O.; Austin, A. J.; Cammi, R.; Pomelli, C.; Ochterski, J. W.; Martin, R. L.; Morokuma, K.; Zakrzewski, V. G.; Voth, G. A.; Salvador, P.; Dannenberg, J. J.; Dapprich, S.; Daniels, A. D.; Farkas, Ö.; Foresman, J. B.; Ortiz, J. V.; Cioslowski, J.; Fox, D. J., *Gaussian 09, Revision A.1, in, Gaussian, Inc., Wallingford CT*, 2009.

8. L. Colon, C. E. Crespo-Hernandez, R. Oyola, C. Garcia and R. Arce, *J. Phys. Chem. B*, 2006, **110**, 15589.
9. C. Nganou, S. D. Kennedy and D. W. McCamant, *J. Phys. Chem. B*, 2016, **120**, 1250.
10. G. W. Doorley, M. Wojdyla, G. W. Watson, M. Towrie, A. W. Parker, J. M. Kelly and S. J. Quinn, *J. Phys. Chem. Lett.*, 2013, **4**, 2739.
11. C. R. Cantor, M. M. Warshaw and H. Shapiro, *Biopolymers*, 1970, **9**, 1059.